Spin-orbit coupling and proximity effects in metallic carbon nanotubes

Piotr Chudzinski
Institute for Theoretical Physics, Center for Extreme Matter and Emergent Phenomena, Utrecht University, Leuvenlaan 4, 3584 CE Utrecht, The Netherlands

(Received 30 April 2015; revised manuscript received 16 July 2015; published 25 September 2015)

We study the spin-orbit coupling in metallic carbon nanotubes (CNTs) within the many-body Tomonaga-Luttinger liquid framework. For a well-defined subclass of metallic CNTs, that contains both achiral zigzag as well as a subset of chiral tubes, an effective low-energy field theory description is derived. We aim to describe systems at finite dopings, but close to the charge neutrality point (commensurability). A new regime is identified where the spin-orbit coupling leads to an inverted hierarchy of minigaps of bosonic modes. We then add a proximity coupling to a superconducting (SC) substrate and show that the only order parameter that is supported within the spin-orbit induced phase is a topologically trivial s-SC.

DOI: 10.1103/PhysRevB.92.115147 PACS number(s): 73.21.Hb, 73.22.Gk, 74.45.+c

I. INTRODUCTION

In the past few years, we have witnessed a renewed interest in superconducting (SC) proximity effects in one-dimensional (1D) systems. The reason why this topic is in the forefront of condensed matter research was the discovery [1,2] that a SC with a topologically nontrivial order parameter is able to support the long sought Majorana surface states [3]. Moreover, it was shown [4] that the nontrivial SC can be artificially created by a proximity coupling of a trivial superconductor with a 1D wire that has a substantial spin-orbit coupling. While the first experimental signatures [5] that such a device can indeed support Majoranas fueled the interest of the community, at the same time questions about the role of disorder [6,7], low-dimensionality breaking, and electron-electron interactions [8] were raised. To avoid at least the first two issues, one may consider a carbon nanotube (CNT), a self-organized, strictly 1D system that nowadays can be produced with ultraclean quality. However, there is still an issue of interactions and moreover one could wonder if the peculiar spin-orbit coupling, that is present in CNT, can produce topologically nontrivial proximity effect. The answer to these questions turns out to be negative and this is one of the main results of this paper.

The price of moving from a simple wire, with e.g. cubic structure, to a CNT is that, in the latter case, one deals with a highly nontrivial mapping between real- and reciprocal-space structures. The low-energy physics of a nanotube can be derived from that of a hexagonal graphene lattice by imposing a quantization condition along the CNT circumference. For concreteness, we consider a CNT with a chiral vector (n,m) such that $(n-m)\mathrm{mod}3=0$. Then, within the subbands that follow from circumferential momentum quantization, there exists a subband which falls very close to the Dirac points K,K' of a graphene reciprocal space. The nanotube is metallic and the vicinities of the two distinct Dirac points are called valleys. More refined analysis includes a curvature-induced shift [9] away from Dirac points Δ_{curv} as well as a spin-orbit coupling [10] that, in the sublattice basis, have both diagonal Δ'_{SO} and nondiagonal Δ_{SO} components [11]. The spin-orbit coupling is a subject of particular interest due to its peculiar nature, with larger nondiagonal Δ_{SO} component.

It is tempting to incorporate the spin-orbit couplings (and Δ_{curv}) on a single-particle level because then their only effect is to change the band structure. So far, all attempts [12,13] to address nontrivial proximity effects in CNT were based on such single-particle framework. However, neglecting the electron-electron interactions $V(q)$ would have been justified only if they were a tiny perturbation added on the top of Δ_{SO} and Δ_{curv}. In reality, $V(q\approx 0)\sim 0.3$ eV and $V(q\approx 2|K|)\sim 10$ meV [14,15] while $\Delta_{\mathrm{curv}}\approx\Delta_{\mathrm{SO}}\leqslant 1$ meV [10,11,16,17] so that one faces exactly the opposite hierarchy of energy scales. Also, at a more fundamental level, a key property of 1D systems is that even upon introducing an infinitesimally small $V(q)$, their low-energy description must be given in terms of collective excitations [18]. A carbon nanotube (CNT) is no exception from this general principle. A well-established fact is that the velocity of charge fluctuations is strongly renormalized [14,15]. This is one manifestation of strong correlations in the physics of CNTs and it implies that a naive refermionization back to the original electrons' framework is not allowed.

It is then an important task to incorporate the effects of spin-orbit coupling into a proper many-body description of CNT. To this end, a few partial problems have already been solved. In Ref. [19], under an assumption that there exists a minigap in the single-particle spectrum, it has been shown that the diagonal component Δ'_{SO} is able to shift velocities and Tomonaga-Luttinger liquid (TLL) parameters of all TLL modes. This shift can be understood [see discussion of Eq. (4)] if one remembers that the onsite component is uniform in space, thus it has a density-density form. Furthermore, a detailed analysis of Δ_{curv} term (and interaction-induced terms of the same form) done for a zigzag tube, exactly at half-filling, was done in Ref. [20]. A crucial assumption was that the system is deep inside a Mott insulating phase. The aim of our work is to go beyond this special case and study a new physics generated by the Δ_{SO} away from commensurability.

A subset of chiral tubes is also covered. Apart from extending the range of validity, this also erases any constraints between Δ_{curv} and Δ_{SO}. For instance, Δ_{curv} can be varied by a tube's twist [21] (not possible for achiral CNTs) or, due to absence of a lattice inversion symmetry, an unprotected Δ_{SO} can be modified by higher-order scattering processes. This versatility allows us to freely tune the parameters of our model.

The paper is organized as follows. In Sec. II we identify a class of chiral tubes where our theory applies and then term by term we introduce a description within the 1D framework.

Section III aims to derive an effective low-energy description in a renormalization group (RG) spirit. It is divided in two parts, a high-energy part Sec. III A, which is dominated by holon behavior, while in Sec. III B dedicated to the lower energies we use adiabatic approximation and focus on gap opening in the spin/valley modes. Then, in Sec. IV, we check the influence of spectral gaps on superconducting proximity effects. Finally, in Sec. V, we discuss an issue of experimental detection of the gaps, an influence of the other symmetry-breaking terms, such as, e.g., valley-mixing term, and other SC orderings proposed for nanotubes. The paper is closed with conclusions, Sec. VI, and two Appendixes that contain estimates for a holon expectation value and for a proximity hybridization with a substrate.

II. CNT AS A TWO-LEG LADDER

The Hamiltonian of a CNT can be written as

$$H = H_0 + H_x + H_{di} + H_{\rm SO}, \tag{1}$$

where H_0 is a TLL Hamiltonian [see Eq. (4)], H_x [Eq. (5)] contains the many-body interactions with large momentum exchange, H_{di} [Eq. (6)] is a dimerization potential introduced to capture $\Delta_{\rm curv}$, in a way following Ref. [20], and the last, new term $H_{\rm SO}$ [Eq. (7)], contains the $\Delta_{\rm SO}$.

The real-space Hamiltonian in fermionic language reads as

$$H_{0+di+{\rm SO}} = \sum_{\vec{r}} \sum_{\vec{d}} (t^{\bar{\sigma}}_{\vec{r},\vec{d}} a^{\dagger}_{\vec{r},\bar{\sigma}} b_{\vec{r}+\vec{d},\bar{\sigma}} + {\rm H.c}), \tag{2}$$

where we have taken a nearest-neighbor hopping on a bipartite lattice. The $a^{\dagger}_{\vec{r}}$ operator creates an electron on the lattice site A with coordinates $\vec{r}$. The summations go over all lattice site positions $\vec{r}$ and all nearest neighbors $\vec{d}$, thus $\vec{d}$ is a linear combination of hexagonal lattice vectors. Due to curvature effects, the hopping parameter, a complex number $t^{\bar{\sigma}}_{\vec{r},\vec{d}}$, is anisotropic in $\vec{r}$ space and spin dependent. On the top of Eq. (2), one adds an electron-electron interaction which has a Coulomb character. In order to extract the low-energy physics, one turns to the reciprocal-space description with a momenta k_x, k_y directed along CNT's axis and circumference, respectively. For a chiral tube, both these axes make a finite angle with a helical line along which the graphene lattice is folded. The resulting band structure is illustrated in Fig. 1. The two cones, that are characteristic of hexagonal lattice, are cut in slices that stem from the circumferential quantization set on k_y.

We put a chemical potential close enough to the Dirac points such that in the following we can restrict ourselves only to the lowest-lying subbands in each of the two valleys. Creation operator $c^{\dagger}_{k,\bar{\sigma}\alpha}$ is assigned to these states, where $\bar{\sigma}$ is a spin index, an index $\alpha = K, K'$, and k is a component of an electron momentum along a CNT, thus 1D physics is implicitly assumed. Then, two Fermi points are present near each Dirac point and this leads to a system with overall four Fermi points. It must be the two-leg ladder model that describes the low-energy physics for this band structure. An exact mapping between real space and $c^{\dagger}_{k}$ has been found for achiral armchair [14] and zigzag tubes [20]. We take a closer look at the later ones as these can accommodate finite $\Delta_{\rm curv}$ and $\Delta_{\rm SO}$, the subject of this study. The zigzag CNT is mapped onto

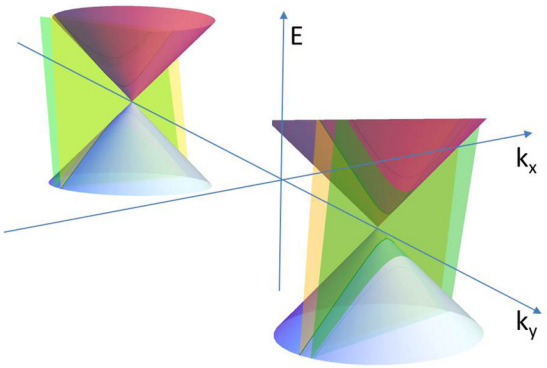

FIG. 1. (Color online) Low-energy band structure of a CNT that falls within the zigzag(like) class. As pointed out in Ref. [14], due to anisotropy of $t^{\bar{\sigma}}_{\vec{r},\vec{d}}$ the cones are slightly shifted away from K, K' points of a reciprocal unit cell. The plane cross sections are due to circumferential quantization condition, only those values of quantized k_y that are closest to Dirac points are shown. On each cone there are two dispersions $E(k_x)$. The mean shift away from Dirac point opens a gap $\Delta_{\rm curv}$, while a split between the two dispersions is proportional to $\Delta_{\rm SO}$. Small tilt of the planes is proportional to $\Delta'_{\rm SO}$, and in Ref. [11] details concerning these spin-orbit effects are given.

a ladder with an interchain $t_\perp = 0$ and this allows us to identify chains (of an abstract ladder) with valleys (of graphene).

The validity of this simple mapping can be extended also onto a subclass of chiral tubes. In a recent work [22], we have showed that it is possible to distinguish a class of tubes defined by a condition $(n-m)/gdc(m,n) {\rm mod} 3 \neq 0$, that have two pairs of Fermi points located around $K_\perp \neq 0$, $K_\parallel \approx 0$, that is similar to the zigzag CNT. In Ref. [22], we considered an infinitely sharp, local chemical potential, an extra term in the Hamiltonian $\sim \mu_0 \delta x - x_0 \rho(x)$ with $\mu_0 \to \infty$ and $\rho(x)$ is an electronic density, a Fourier transform of $\sum_k c^{\dagger}_k c_{k+q}$. For the zigzaglike tubes, a response to such potential is a reflection matrix that is strictly diagonal in the valley space. From this it follows that an operation $c^{\dagger}(x = x_0)|\Psi_k\rangle$ (where $|\Psi_k\rangle$ is an eigenstate) is diagonal in the valley space. We apply creation operation infinitely many times along a CNT to find that $\int dx\, c^{\dagger}(x)|\Psi_k\rangle$ is also diagonal in valley space which implies that a valley ≡chain description, with $t_\perp = 0$, should be valid for these chiral tubes, at least in the regime close to the Dirac points ($k_\parallel \approx 0$) which is of interest in this study. To quantify the criterion, by analogy with commensurate-incommensurate transition [23], we notice a competition between the interchain interaction terms $\sim g_{ic} \cos \phi_{\rho-}$ [see following for definition of bosonic fields and Eq. (5)] and the interchain hopping (present for $k_\parallel \neq 0$) that upon bozonization gives a term $\sim t_\perp \cos \theta_{\rho-}$. These bosonic expressions, that contain two canonically conjugated fields, suggest that the following criterion for $k_\parallel$ can be given $t \sin(k_\parallel a) < g_1$. Substituting numerical values, this implies that our reasoning can be safely applied when the doping $\delta < 0.03$. The fact that a CNT can be described as valley ≡chain ladder is enough to apply to the results of this work.

We go directly to the bosonization description of the lowest subband fermions. We follow a standard procedure. First, one extracts the long-wavelength behavior around the Fermi

points:

$$\bar{\psi}_{\bar{\sigma}\alpha}(x) = \exp(ik_F x)\psi_{R\bar{\sigma}\alpha}(x) + \exp(-ik_F x)\psi_{L\bar{\sigma}\alpha}(x),$$

where we have written the formula in terms of a real-space field $\bar{\psi}_{\bar{\sigma}\alpha}(x)$ which is an eigenvalue of the second quantization operators $c_{\bar{\sigma}\alpha}(x)$ (Fourier transform of $c^{\dagger}_{k,\bar{\sigma}\alpha}$) in the Fock space of the coherent states. Then, one focuses on the slow components of the fluctuations around Fermi points and introduces the collective bosonic fields:

$$\psi_{R,L\bar{\sigma}\alpha}(x) = \kappa_{R,L\bar{\sigma}\alpha}\frac{1}{2\pi a}\exp\{i[\phi_{\bar{\sigma}\alpha}(x) \pm \theta_{\bar{\sigma}\alpha}(x)]\}, \quad (3)$$

where $\kappa_{R,L\bar{\sigma}\alpha}$, the Klein factors, ensure proper anticommutation relations. The collective fields can be also expressed directly through the real-space density operator defined before (for the valley-diagonalization argument), for instance, $\phi_{\bar{\sigma}\alpha}(x) = -\pi\nabla\rho_{\bar{\sigma}\alpha}(x)$. Finally, one turns to a total/transverse basis by a transformation

$$\begin{aligned}\phi_{\rho\pm} &= \tfrac{1}{2}(\phi_{1\uparrow} + \phi_{1\downarrow} - \phi_{2\uparrow} - \phi_{2\downarrow});\ \phi_{\sigma\pm}\\ &= \tfrac{1}{2}(\phi_{1\uparrow} + \phi_{1\downarrow} - \phi_{2\uparrow} - \phi_{2\downarrow}).\end{aligned}$$

Four collective modes ϕ_ν (and canonically conjugate θ_ν) are present: total/transverse charge/spin modes ($\nu = \rho\pm,\sigma\pm$). The total charge mode $\rho+$ is sometimes called a holon as it contains an electric charge of a hole, while the other three modes are neutral and contain the spin/valley component. With these bosonic modes defined, we can now write each part of Eq. (1). The H_0 reads as

$$H_0[\phi_\nu] = \sum_\nu \int \frac{dx}{2\pi}\left[(v_\nu K_\nu)(\partial_x\theta_\nu)^2 + \left(\frac{v_\nu}{K_\nu}\right)(\partial_x\phi_\nu)^2\right]. \quad (4)$$

The main advantage of working in the bosonization framework is that an entire $V(q \approx 0)$ part of interactions is already included in Eq. (4). Since in CNTs the interactions have a long-range Coulomb character, the small momentum exchange interactions are much larger than those with large momentum exchange. The Coulomb interactions bosonize as

$$H_{\rm Cou} = \frac{2e^2}{\pi}\int dx \int dx' V(r-r')\partial_x\phi_{\rho+}(x)\partial_{x'}\phi_{\rho+}(x').$$

Clearly, only the total charge mode (holon) is affected. Because of this, the holons' velocity $v_{\rho+}$ can be up to five times larger than V_F, while $K_{\rho+}$ can be as small as 0.25. Velocities of all the other so-called neutral modes remain $\approx V_F$.

The large momentum exchange part of electron-electron interactions, where $V(q \approx |K|)$, or in other words the part that cannot be written in a density-density form that is $\neq \int dx \int dx' \rho(x)\rho(x')$, adds several nonlinear terms:

$$\begin{aligned}H_x = \frac{1}{2(\pi a)^2}\int dr\, g_3 &\cos(2\phi_{\rho+} - 2\delta x)[\cos(2\phi_{\rho-})\\ &+ \cos(2\phi_{\sigma+}) + \cos(2\phi_{\sigma-}) + \cos(2\theta_{\sigma-})]\\ &- g_{1c}\cos(2\phi_{\rho-})\cos(2\phi_{\sigma+}) - g_{2c}\cos(2\phi_{\rho-})\\ &\times \cos(2\phi_{\sigma-}) + g_{1a}\cos(2\phi_{\sigma+})\cos(2\theta_{\sigma-}) + g_{\|c}\\ &\times \cos(2\phi_{\rho-})\cos(2\theta_{\sigma-}) + g_1\cos(2\phi_{\sigma+})\cos(2\phi_{\sigma-}), \quad (5)\end{aligned}$$

where the backscattering terms, with spin and/or valley index change in the process, are indicated as $g_{1,2i}$. We use notation from Ref. [24] and convention for the Klein factors as in Refs. [15,24]. The only difference is that Ref. [24] is dedicated to two-leg ladders with large $t_\perp$ (more customary case) while here $t_\perp = 0$ but a finite interchain interaction $V_\perp$ is present. To transfer between the two models it is enough to make an interchange $\cos 2\phi_{\rho-} \Leftrightarrow \cos 2\theta_{\rho-}$ in Eq. (5). Terms $\sim g_3$ in Eq. (5) are umklapp scattering terms which transfer two left movers into right movers (or vice versa). This requires commensurability with the lattice, obeyed at half-filling, while at finite doping δ these are gradually suppressed.

Additional terms, dimerization and spin-orbit coupling, are present because the C_3 symmetry of the underlying graphene lattice is broken upon wrapping. A σ^*-π^* hybridization, induced by wrapping, changes the hopping amplitude along the tube circumference and this shifts the position of the Dirac points [14]. The lowest-energy subbands are defined independently by the quantization condition along the tube circumference, so they are now shifted with respect to the new Dirac cones. This effectively results in an opening of a so-called *minigap* in the spectrum, the $\Delta_{\rm curv}$. As it was proven in Ref. [20] this effect can be grasped by introducing a dimerization potential into the effective 1D Hamiltonian of CNT [Eq. (1)]. Such a term, the Peierls term, is well known in 1D systems, it is exactly solvable via Bogoliubov transformation in the particle-hole channel, and leads to a gap opening in the single-particle spectrum. In bosonization language, it reads as [20]

$$\begin{aligned}H_{di} = \frac{1}{2\pi a}\int dx\, g_d[&-\cos(\phi_{\rho+} - \delta x)\cos\phi_{\rho-}\\ &\times \cos\phi_{\sigma+}\cos\phi_{\sigma-} - \sin(\phi_{\rho+} - \delta x)\sin\phi_{\rho-}\\ &\times \sin\phi_{\sigma+}\sin\phi_{\sigma-}], \quad (6)\end{aligned}$$

where $g_d = V_{di}/V_F$ generates minigaps $\Delta_{\rm curv}$ at K, K' points. From the Bogoliubov transformation, done for an alternating potential in a single-particle limit, we know that in the lowest order the relation is simple $V_{di} = \Delta_{\rm curv}$. However, V_{di} incorporates also further terms, the staggered potential terms that are produced in the course of the RG flow [20]. The sole term V_{di} [Eq. (6)], written in bosonization language, contains a sort of "frustration": there is a competition between terms perfectly compensating each other. Sines and cosines wish to lock ϕ_ν fields at different minima. When V_{di} dominates the physics, then the bosonic framework is inappropriate, instead one should turn back to the original fermions (to obtain the Peierls transition). But, this simple prescription does not work if there are other terms, such as electron-electron interactions, present as well. Then, it is necessary to write H_{di} (and $H_{\rm SO}$) in the bosonization language in order to take advantage of the adiabatic approximation [20,25,26] and separate out the influence of the fast $\phi_{\rho+}$ field. In Ref. [20] the "frustration" problem was solved by considering a regime dominated by the umklapp scattering (deep inside the Mott phase) which favors $\cos\phi_{\rho+}$ and then also other cosines automatically follow. Following, we show a different mechanism that is able to lift the frustration.

The spin-orbit coupling shifts band dispersions away from the Dirac points by an amount that depends on the spin/valley degree of freedom of a fermion, in an opposite direction for electrons with opposite helicities [16]. Alternatively, this

phenomenon can be seen as a spin-dependent variation of a minigap in the spectrum around the point where bonding and antibonding bands used to cross in the tight-binding model. As a result, in the single-particle picture, $\Delta_{\rm SO}$ adds a spin-/valley-dependent component to the minigaps (see Fig. 1). By reasoning along the same lines as for the curvature term, this can be interpreted as an extra spin-valley-dependent single-particle backscattering. The $\Delta_{\rm SO}$ term is then expected to have a form similar to Eq. (6), with the only difference that the left/right mixing term now involves the z-Pauli matrices in spin and valley spaces [12]:

$$\hat{O}_{\rm SO} \sim c^\dagger_{LK\uparrow}c_{RK\uparrow} - c^\dagger_{LK'\uparrow}c_{RK'\uparrow} - c^\dagger_{LK\downarrow}c_{RK\downarrow} + c^\dagger_{LK'\downarrow}c_{RK'\downarrow}.$$

The spin-orbit coupling is expressed in the spin-valley basis because of the intricate topological origin of the effect [10,11,16,17]: electrons of opposite valleys are precessing along the helical lines of opposite twist. However, we have established that, within our effective two-leg ladder description, the valley degree of freedom can be associated with the chain index. Then, in Eq. (3), $\alpha = K, K'$ and thanks to that $\hat{O}_{\rm SO}$ has a simple bosonized expression. Finally, the spin-orbit term that is off diagonal in the sublattice space asks to choose a bond (not an onsite) operator to be Hermitian. These few constraints are enough to deduce the following form of spin-orbit term $\Delta_{\rm SO}$ in the bosonic language:

$$H_{\rm so} = \frac{1}{2\pi a}\int dx\, g_{\rm SO}[-\cos(\phi_{\rho+} - \delta x)\cos\phi_{\rho-}\cos\phi_{\sigma+} \times \cos\phi_{\sigma-} + \sin(\phi_{\rho+} - \delta x)\sin\phi_{\rho-}\sin\phi_{\sigma+}\sin\phi_{\sigma-}]. \tag{7}$$

One immediately notices that thanks to an opposite sign of the two terms in Eq. (7), the $g_{\rm SO}$ is able to lift the frustration present in the sole H_{di}.

III. RG TREATMENT OF COSINE TERMS

As usual in the RG procedure, we inspect how the parameters of the Hamiltonian are effectively changing upon integrating out high-energy degrees of freedom. The RG flow is divided in two stages: the first when the doping is negligible and the system flows like if it was at commensurate filling, the second when doping is significant and only the backscattering terms in Eq. (5) should be kept.

A. High-energy RG flow

The first stage of RG flow stops at energy scale Λ' that is defined by the condition $\delta[\Lambda'] = 1$. Above this energy RG is dominated by the umklapp and dimerization/spin-orbit terms whose perturbative, single-loop, RG equations read as

$$\dot{g}_3 = 3g_3(1 - K_{\rho+}), \tag{8}$$

$$\dot{g}_{d,\rm SO} = g_{d,\rm SO}[2 - (K_{\rho+} + K_{\rho-} + K_{\sigma+} + K_{\sigma-})/4], \tag{9}$$

where, in the first equation, we used the fact that $K_{\rho-} \approx K_{\sigma+} \approx K_{\sigma-} \approx 1$, otherwise three different equations for three different umklapp channels would need to be given. The reason why Eq. (8) dominates is because in CNT, in the UV limit, a relevant parameter range is $0.2 < K_{\rho+} \ll 1$, thus, one can safely assume $|K_{\rho+} - 1| \gg |K_{\nu\neq\rho+} - 1|$ and then all terms that contain the $\phi_{\rho+}$ mode are much more relevant than others. The umklapp has a scaling dimension $d_3 = 1 - K_{\rho+}$ while the g_d and $g_{\rm SO}$ are even more relevant with $d_d = 1.25 - K_{\rho+}/4$.

The RG flow of other nonlinear terms is determined by the following equations:

$$\dot{g}_{1c} = g_{1c}[2 - (K_{\rho-} + K_{\sigma+})], \tag{10}$$

$$\dot{g}_{2c} = g_{2c}[2 - (K_{\rho-} + K_{\sigma-})], \tag{11}$$

$$\dot{g}_{1a} = g_{1a}[2 - (K^{-1}_{\sigma-} + K_{\sigma+})], \tag{12}$$

$$\dot{g}_{\|c} = g_{\|c}[2 - (K^{-1}_{\sigma-} + K_{\rho-})], \tag{13}$$

$$\dot{g}_1 = g_1[2 - (K_{\sigma-} + K_{\sigma+})]. \tag{14}$$

While this flow is much slower in the first stage of RG, in the second stage of RG, Eq. (10) becomes the driving force.

The TLL parameters are also renormalized:

$$\dot{K}_{\rho+} = -\tfrac{1}{2}K^2_{\rho+}\big(4g_3^2 + g_d^2 + g_{\rm SO}^2\big)J_0(\delta), \tag{15}$$

$$\dot{K}_{\rho-} = -\tfrac{1}{2}K^2_{\rho-}\big[J_0(\delta)\big(g_3^2 + g_d^2 + g_{\rm SO}^2\big) + g_{1c}^2 + g_{2c}^2 + g_{\|c}^2\big], \tag{16}$$

$$\dot{K}_{\sigma+} = -\tfrac{1}{2}K^2_{\sigma+}\big[J_0(\delta)\big(g_3^2 + g_d^2 + g_{\rm SO}^2\big) + g_{1c}^2 + g_{1a}^2 + g_1^2\big], \tag{17}$$

$$\dot{K}_{\sigma-} = -\tfrac{1}{2}K^2_{\sigma-}\big[J_0(\delta)\big(g_d^2 + g_{\rm SO}^2\big) + g_1^2 + g_{2c}^2\big] + g_{1a}^2 + g_{\|c}^2, \tag{18}$$

where $J_0(\delta)$ is a Bessel function of the first kind (we take UV cutoff equal to one).

The bare (initial) amplitudes of the exchange terms in Eq. (10) are small but finite and were thoroughly calculated in Ref. [15]. In that language, $g_{1c} = g_1 = f$, $g_{2c} = b - f$, and $g_{1a} = g_{\|c} = b$, where b, f are amplitudes of large momentum scattering processes computed on a microscopic CNT lattice for armchair tube. The estimate $b, f \approx (0.05, 0.1)V(q = 0) \approx (0.005, 0.01)V_F$ was given and in our chiral case we are likely to be close to the upper limit since in a less symmetric lattice certain cancellation between real-space Coulomb interactions are not exact. On the top of it, in our nonarmchair case, there is a contribution from a coupling between orbital momenta of two electrons. It enhances $g_{1c}, g_1, g_{\|c}$ (a ferro-orbital configuration of initial orbital momenta μ_o implies that the two carriers will repel each other) and reduces g_{2c}, g_{1a} (an antiferro-orbital configuration of initial orbital momenta μ_o). In CNTs, μ_o can be an order of magnitude larger [27] than μ_B which makes this unusual contribution to electron-electron interactions worth considering. To estimate it we can compare it with $\Delta_{\rm SO} \approx |\mu_o||\mu_B| \leqslant 1$ meV. $\Delta_{\rm SO}$ originates from similar mechanism, an interaction between μ_o and μ_B as a carrier moves along a helical line of a CNT. The umklapp terms correspond to terms with even larger momentum exchange, thus their initial (UV) amplitudes are smaller for the Coulomb-type interactions. Moreover, their amplitude is further suppressed by a finite doping and this suppression is two times faster than for the V_{di} amplitude.

Our study is dedicated to the case of a finite doping. Since in the later part of the paper the SC proximity effects are

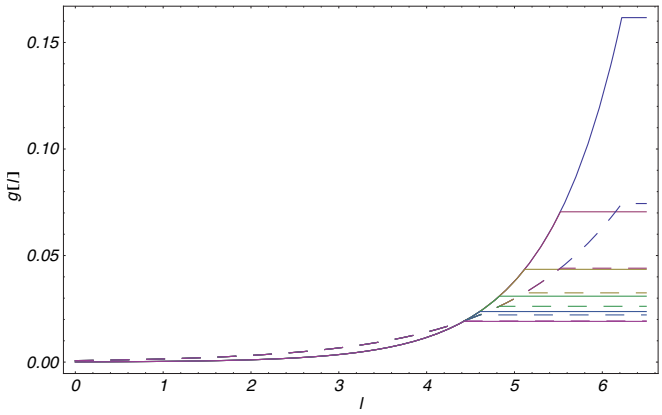

FIG. 2. (Color online) The RG flow of couplings that are violently relevant in the first stage of RG: the umklap (dashed lines) and dimerization (solid lines) terms. Different doping levels are shown by different color code (from top to bottom): from $\delta = 0.002$ to 0.012 with intervals 0.002. One notices that in a point when flow stops, thus for $l = \Lambda'$ the dimerization term is always stronger at finite dopings even though we started with $g_d = g_{\rm SO} = 0.0001$ and $g_3 = 0.0007$ (and $K_{\rho+} = 0.25$).

considered, we must take a model with a nonzero conductance on an interface with a substrate, thus a model with a constant chemical potential. Then, the doping is not a constant but a renormalizable quantity that competes with interactions. This effect we incorporate in the following RG equation:

$$\dot{\delta} = \delta - \left(3g_3^2 + g_d^2 + g_{\rm SO}^2\right) J_1(\delta), \tag{19}$$

where $J_1(\delta)$ is a Bessel function of the first kind. The RG flow of δ (in the first stage of RG) can produce two outcomes: (i) $\delta[l]$ rapidly grows and when $\delta[l] \sim 1$ then this first stage of RG must be stopped and g_3 terms in Eq. (5) and g_d (and $g_{\rm SO}$) terms Eqs. (6) and (7) effectively drop out of the problem because the integrands in Eqs. (5)–(7) contain rapidly oscillating terms; (ii) $\delta[l]$ rapidly drops to zero then the system flows to a Mott or Peierls physics, where a competition between g_3 and g_{di} (and $g_{\rm SO}$) determines the low-energy properties. Case (ii) can be realized only when $\delta[\Lambda] < g_i^2$ which for CNTs translates into extremely small doping levels. Nevertheless, for a finite $\delta[l]$ during RG, this competition persists and since the dimerization is less affected by doping, then this phase should expand. Crucially, as we show later in Sec. III B 1, the nature of the "dimerized" phase changes when the energy scale Λ' is of the same order or smaller than $\Delta_{\rm SO}$.

Close to commensurate filling, for a parameter range that is relevant for a CNT, we identify quite a broad regime where g_d (and $g_{\rm SO}$) dominate over g_3 terms. We analyze several RG flows for initial parameters: $g_d = g_{\rm SO} = 0.0001$, $g_3 \in (0.0001, 0.001)$, $K_{\rho+} \in (0.25, 0.35)$ (these values are relevant for CNTs), and $\delta[l = 0] \in (0.001, 0.012)$. Some examples of RG flows for different δ are given in Fig. 2. We observe that both terms grow and, in a chosen range of parameters, the dimerization term is always the dominant one, even if one starts with (an overestimated) ratio $g_3[\Lambda]/g_d[\Lambda] \simeq 10$. The flow stops for $l_1 \in (5.5, 7)$ which taking initial UV cutoff $\Lambda = 1.5$ eV translates into an energy scale $\Lambda' \sim 10^{-3}$ eV that is comparable with the bare $\Delta_{\rm SO}$. The values reached by g_3 and g_d (and $g_{\rm SO}$) at Λ' are substantial $g_3 < g_d \sim 10^{-1}$ (see Fig. 2) but still below $\sim 10^0$, thus gaps are not open yet. While these terms drop out of RG but in the following should be considered as a substantial perturbation.

B. Physics at energies below $\Lambda' \sim 1$ meV

1. Antiadiabatic approximation

We restrict ourselves to $H = H_0 + H_{di} + H_{\rm SO}$. At Λ' we reanalyze the theory using the adiabatic approximation [25]. To be precise, we use an antiadiabatic version of it to focus on the physics of three neutral modes. Following Ref. [26], we separate out the fast $\phi_{\rho+}$ field using an auxiliary variable $\eta(x) = \arctan[(\sin\phi_{\rho-}\sin\phi_{\sigma+}\sin\phi_{\sigma-})/(\cos\phi_{\rho-}\cos\phi_{\sigma+}\cos\phi_{\sigma-})]$. After shifting the field $\tilde{\phi}_{\rho+}(x) \to [\phi_{\rho+}(x) + \delta x] + \eta(x)$, the action is separable. Then, for the fast field we obtain a sine-Gordon model

$$H_{\phi_{\rho+}} = H_0[\phi_{\rho+}] - \int dr\, M[\phi_{i\neq\rho+}] \cos[\tilde{\phi}_{\rho+}(x)], \tag{20}$$

where the mass term

$$M[\phi_{i\neq\rho+}] = [V_{\rm SO}(l) + V_{di}(l)]|_{\Lambda'} \sqrt{1 + \sum_{\nu\neq\iota} \cos 2\phi_\nu \cos 2\phi_\iota}$$

can be obtained using identities $\arctan[\sin(\alpha/\beta)] = \alpha/(\alpha^2+\beta^2)^{-1}$ and $(\sin\phi_{\rho-}\sin\phi_{\sigma+}\sin\phi_{\sigma-})^2 + (\cos\phi_{\rho-}\cos\phi_{\sigma+}\cos\phi_{\sigma-})^2 = 1 + \sum_{j\neq i}\cos 2\phi_j \cos 2\phi_i$. While writing Eq. (20) we neglect terms $\sim\eta(x)$ (and higher powers) and derivatives $\sim\partial_t\eta(x)$, which is justified in the adiabatic limit [slow $\eta(x)$] and in the presence of substantial $V_{\rm SO}$ [then $\eta(x) \to 0$ is justified]. The $V_{\rm SO}$, as written in Eq. (7), favors cosines' over sines' minima and thus provided $V_{\rm SO} \sim \Lambda'$ we tend to a well-defined limit $\eta \to 0$, variations of η field are gradually suppressed.

2. Effective Hamiltonian for the slow fields

For the slower fields we proceed by integrating out the $\tilde{\phi}_{\rho+}$. At energies $\sim\Lambda'$, Eq. (20) is a sine-Gordon model, thus $\langle\cos[\tilde{\phi}_{\rho+}(x)]\rangle|_{\omega=\Lambda'} \neq 0$ (see Appendix for details). Then, upon expanding $M[\phi_{i\neq\rho+}]$ we arrive at an emergent nonlinear term

$$H_{\tilde{d}i}[\phi_{i\neq\rho+}] = -g_d'\{\cos(2\phi_{\rho-})\cos(2\phi_{\sigma+}) + \cos(2\phi_{\sigma-})[\cos(2\phi_{\sigma+}) + \cos(2\phi_{\rho-})]\}, \tag{21}$$

where $\tilde{g}_d \sim g_d\langle\cos[\tilde{\phi}_{\rho+}(x)]\rangle$ and in the lowest approximation the expectation value is proportional to the symmetry-breaking term $\langle\cos[\tilde{\phi}_{\rho+}(x)]\rangle \sim V_{\rm SO}$. In the sign convention we use both Hamiltonians (6) and (21) are minimized by the same combination of locked neutral fields, thus validating our mapping. Equation (21) should be combined with the backscattering part of H_x [Eq. (5)]. The following perturbation to $H_0[\phi_{\nu\neq\rho+}]$

emerges:

$$H_{\tilde{x}} = -\tilde{g}_{1c}\cos(2\phi_{\rho-})\cos(2\phi_{\sigma+}) + \cos(2\phi_{\sigma-})[-\tilde{g}_{2c}\cos(2\phi_{\rho-}) + \tilde{g}_1\cos(2\phi_{\sigma+})] + \cos(2\theta_{\sigma-})[\tilde{g}_{1a}\cos(2\phi_{\sigma+}) + \tilde{g}_{\|c}\cos(2\phi_{\rho-})]. \quad (22)$$

The initial parameters for second stage of RG flow (we take a new UV cutoff Λ') are determined by the values obtained in the end of the first stage. The RG flow of H_x is a BKT flow with the parameters that fall close to the negative separatrix [15] [the SU(2) invariant line on the g-K plane, with the RG flowing straight away from the critical point]. Then, in the first RG stage, $g[l]/V_F = g[\Lambda]/V_F/(1 - g[\Lambda]l)$ and one finds that $g_{1c}[\Lambda'], g_{2c}[\Lambda'], g_1[\Lambda'] \sim 10^{-2}$. However, some of the $g_i'[\Lambda']$ terms are larger because they contain also $g_d[\Lambda']$ contribution (which is significant even when multiplied by $\langle\cos\tilde{\phi}_{\rho+}\rangle|_{\omega=\Lambda'}$). To be precise: $\tilde{g}_{1c}[\Lambda'] = g_{1c}[\Lambda'] + \tilde{g}_d[\Lambda']$, $\tilde{g}_{2c}[\Lambda'] = g_{2c}[\Lambda'] + \tilde{g}_d[\Lambda']$, $\tilde{g}_1[\Lambda'] = g_1[\Lambda'] - \tilde{g}_d[\Lambda']$, while all other terms are not affected. As for the TLL parameters, in the first part of the RG flow the umklapp, dimerization, and spin-orbit terms all involve $\sim\cos(\phi_{\rho-})$. As a result, the RG flow changes the TLL parameter $K_{\rho-}$ downwards (already initially, at $l = \Lambda_0$, this term is shifted slightly below $K_{\rho-} = 1$ by interactions [15] as well as $\Delta_{\rm SO}'$ [19]), same holds for $K_{\sigma+}$. Thus, we conclude that for $g_{1c}\cos(\phi_{\sigma+})\cos(\phi_{\rho-})$ term we make a shift upwards along the negative separatrix, that is, both g_{1c} and $1 - K_{\rho-}$ change upwards. Since close to the separatrix the gap $\Delta = \Lambda\exp(-V_F/\tilde{g}_{1c})$, the dependence is exponential. Taking quite a conservative estimate that both $g_{1c}[\Lambda']$ and $\tilde{g}_d[\Lambda']$ are of the same order, we find that the exponent is reduced by a factor of 2 in comparison with Ref. [15]. This leads to much enhanced gaps $\Delta_{\rho-,\sigma+} \sim 0.1$ meV. Numerical (RG) calculations confirm this finding: $g_{1c}'[l'] = 1$ already for $l' \approx 2$. A gap opens in the spectrum of the two bosonic modes $\phi_{\sigma+}$,$\phi_{\rho-}$. The fields are locked at an energy minima $\phi_{\sigma+} = 0$, $\phi_{\rho-} = 0$. The gap value is equal to the mass of a soliton of the sine-Gordon model $M_{\rho-,\sigma+} = 2\sqrt{2\tilde{g}_{1c}u_{\rho-}/\pi K_{\rho-}}$, from this $M_{\rho-,\sigma+} \approx 0.1$ meV. The two estimates coincide.

The RG flow of $\sigma-$ mode is more difficult to follow. In H_x [Eq. (5)] we find competing $\cos(\phi_{\sigma-})$ and $\cos(\theta_{\sigma-})$ terms which exactly compensate each other, also in the lowest-energy sector when some modes acquire gaps. Moreover, this implies that $dK_{\sigma-}/dl \approx 0$, while to begin with $K_{\sigma-} = 1$ and even accounting for the diagonal spin-orbit coupling [19], the $\Delta_{\rm SO}'$ does not move $K_{\sigma-}$ from the marginal value $K_{\sigma-} = 1$. Thus, we conclude that this mode is in a self-dual point, at least within the manifold of interaction terms we decided to take into account. Usually, such a situation is treated by employing refermionization [28], then separating real/imaginary parts as Majorana fermions, e.g., $\xi_{0,i} = \mathrm{Re}[\exp\phi_{\sigma-}(x_i)]$, and finally using fusion rules to map the Hamiltonian onto a doublet of quantum Ising chains $H_0[\sigma-] + H_{\tilde{x}}[\sigma-] = \sum_{l=0,1}\sum_i \sigma_{l,i}^z\sigma_{l,i}^z + h\sigma_{l,i}^x$ with order/disorder operators $\sigma_{0,1}$,$\mu_{0,1}$ defined as $\xi_{0,i} = \sigma_{0,i}\mu_{0,i}$. In Refs. [15,25] the procedure was used in the context of CNTs. The self-dual point is equivalent, in the Ising model language, to σ_1 chain passing through criticality. The other Ising chain is always gapped and, by accounting for a negative sign of the mass term, we deduce that the order Ising operators σ_0 have a finite amplitude, which means that $\sin\phi = 0$ and $\sin\theta = 0$, while both respective cosines are nonzero. This does not allow us to identify the unique ground state, but only to narrow down the possibilities. Since $K_{\rho+} < 1$ it shall be density wave (DW) ordering, either intravalley charge density wave (CDW) or intravalley spin density wave (SDW), with either bond or onsite character. One must remember that there are other ordering possibilities, e.g., squared order parameters, with higher periodicities, which may be dominant when $K_{\rho+} < 0.25$. Furthermore, since self-duality is not protected by any symmetry, one cannot exclude that due to some extremely tiny perturbation, not accounted in our generic model, a gap in $\phi_{\sigma-}$ actually opens. However, this depends on the finer details of a CNT under consideration and describes physics that takes place at energies $\sim 10^{-9}$ eV or below [15], so we refrain from its further analysis here.

Even though the exact ground state remains elusive, the larger gaps $M_{\rho-}, M_{\sigma+}$ that certainly open provide sufficient conditions to determine the allowed proximity effect.

IV. PROXIMITY EFFECTS

The inverted hierarchy of gaps plays an important role in the proximity effect. This is because usually the coupling with the substrate and the superconducting gap (on the surface) are smaller than $M_{\rho-,\sigma+}$. In the Appendix, we give a brief description of the hybridization, in the fermionic language. To understand how these microscopic considerations are linked with many-body TLL theory, one must sum over all sites of the CNT within a unit cell, turn to collective fields, and then express the result in the two-leg ladder basis. This is a well-established procedure; we follow Ref. [25] to find that the singlet SC order operators in a zigzag(like) CNT are

$$\hat{O}_s^{\rm SC} \sim \exp(\imath\theta_{\rho+})[\cos\phi_{\rho-}\cos\phi_{\sigma+}\cos\theta_{\sigma-} + \imath(\sin\leftrightarrow\cos)], \quad (23)$$

$$\hat{O}_m^{\rm SC} \sim \exp(\imath\theta_{\rho+})[\cos\phi_{\rho-}\sin\phi_{\sigma+}\sin\theta_{\sigma-} + \imath(\sin\leftrightarrow\cos)]. \quad (24)$$

The first one, $\hat{O}_s^{\rm SC}$, corresponds to a purely local tunneling process (a pair is created on one site) and thus it is more likely to occur in type-II superconductor (short coherence length), than $\hat{O}_m^{\rm SC}$ when a pair is created nonlocally (with different phase on adjacent sites). Both $\hat{O}_{s,m}^{\rm SC}$ have a scaling dimension $d_\Delta = 2 - (3 + K_{\rho+}^{-1})/4$, thus they are relevant for $K_{\rho+} > 0.2$. This holds when we assume $K_\nu = 1$ for $\nu \neq \rho+$, accounting for the fact that actually (in the low-energy limit) $K_{\rho-} < 1$ changes the condition to $K_{\rho+} > 0.25$. It is likely that the condition $K_{\rho+} > 0.25$ is fulfilled when a CNT lies on a conducting substrate which provides the screening for Coulomb interactions and thus reduce their range. The relevance of $\hat{O}_{s,m}^{\rm SC}$ does not matter if one is deep inside the Mott phase and a large gap in the $\phi_{\rho+}$ field causes strong fluctuations of $\theta_{\rho+}$, thus suppressing any SC proximity effect. This would be the case in a system described in Ref. [20] where the dimerization term H_{di} was governed by the Mott gap. In this work, we have found another mechanism where the field $\eta(x)$ is locked by the symmetry breaking $H_{\rm SO}$, and thanks to that the field $\theta_{\rho+}$ is not randomly fluctuating

at the lowest energies. Considering the relevance of the SC proximity now makes sense.

The presence of $M_{\rho-}, M_{\sigma+}$, or to be more precise the field configuration they impose, sets a constraint on the allowed proximity effect. If we disregard the $\sigma-$ mode for a moment, then we find that there exists one SC order parameter which is compatible with the locked fields $\langle\phi_{\rho-}\rangle = 0$ and $\langle\phi_{\sigma+}\rangle = 0$. It is the s-SC that is also the most likely candidate from the microscopic viewpoint. This order has a topologically trivial character. The other O_m order parameter is suppressed because it requires to lock the $\phi_{\sigma+}$ field at the other minimum: $\phi_{\sigma+} = \pi/2$. The triplet order parameters are exponentially suppressed because they involve the $\theta_{\sigma+}$ field which is canonically conjugate to the locked $\phi_{\sigma+}$.

As for the $\sigma-$ mode, there are two options:

(i) The mode stays on a self-duality point: then $\cos\theta_{\sigma-}$ has a finite expectation value and s-SC is allowed.

(ii) Ultimately the gap opens, at much reduced energies: this will be most likely a gap in the $\phi_{\sigma-}$ field $m_{\sigma-}$. It could suppress the s-SC proximity effect at the lowest energies. One way to overcome it is to take a sufficiently large amplitude of the proximity-induced gap $\Delta_s^{\rm SC} > m_{\sigma-}$. Thanks to a huge difference of energy scales between the different masses, the 1D character of the system will be still protected by $M_{\rho-}$. The induced transition to the s-SC state shall have the Ising character [29] (one of Ising disordered operators μ_1 acquires a finite value at the cost of the Ising ordered operator σ_1).

In either case, only the topologically trivial s-SC is allowed. The Majorana surface states are never allowed to occur.

V. DISCUSSION

A. Size of the spectral gap and the means of its detection

The estimate for spectral gaps that we have given in Sec. III B is rather conservative, valid for a CNT embedded in a good dielectric, for instance, a CNT suspended in vacuum. By introducing an extra screening, for example, by placing a tube on a superconducting substrate or within a multiwall CNT, one makes electron-electron interactions more local. In reciprocal space, this increases the large momentum exchange component of electron-electron interactions $V(q \approx 2K)$. Then, the bare amplitudes of the backscattering terms g_i in Eq. (5) can grow substantially. Moreover, as we indicate in the context of the proximity effect, placing the tube on an appropriately chosen substrate may introduce additional periodic potentials that cause backscattering and adds up with g_d and $g_{\rm SO}$. The magnitude of gaps depends on particular experimental realizations and in some circumstances it can be detectable already at energies $\sim$1 meV.

One possibility to detect the $M_{\rho-}, M_{\sigma+}$ is to study the Knight shift and relaxation rate of NMR signal. The temperature dependence shall be a power law but at the energy scale corresponding to the gap one should observe a change of an exponent, such an effect was indeed experimentally [30,31] observed but its origin was unclear. In our mechanism, for instance for the Knight shift we predict a change from $(K_{\sigma+} + K_{\sigma-})/2$ to $K_{\sigma-}/2$. Moreover, a known feature of the spin-valley-dependent split $V_{\rm SO}$ is that it can be varied by applying an external magnetic field [16,27]. Since both $M_{\rho-}$ and $M_{\sigma+} \sim \tilde{g}_d \sim V_{\rm SO}$, and the spin-/valley-dependent part of the split in a single-particle dispersion can be varied by a magnetic field directed along a tube, then an anisotropic magnetic field dependence of spectral gaps can be taken as a hallmark of their many-body origin.

B. Relation to SC order parameters proposed for CNTs

The $\hat{O}_s^{\rm SC}$ in the same form as Eq. (23) was also proposed by Egger [15]. The fermionic expression, in the reciprocal space, for superconducting order parameter that we invoked $\hat{O}_s^{\rm SC}$ reads as

$$\hat{O}_s^{\rm SC} = (c^\dagger_{kK\uparrow} c^\dagger_{-kK'\downarrow} + \text{H.c.}) - (\uparrow\leftrightarrow\downarrow)$$

and it is equivalent to an interchain ordering as derived in a seminal paper [32]. In the last paper it is called d-SC, but this should not lead to any misunderstanding since we define order parameters for real-space hexagonal lattice, what is $\hat{O}_d$ for a square ladder is not necessarily d wave for other underlying crystal lattice. A detail description of the symmetry properties for a bi-layer graphene interface is given in Ref. [33] where a table of characters for the local $\hat{O}_s^{\rm SC}$ [Eq. (23)] as well as the nonlocal $\hat{O}_m^{\rm SC}$ [Eq. (24)] were found. In particular, it was explicitly shown that only the $\hat{O}_m^{\rm SC}$ may contain topologically nontrivial SC order.

Furthermore, one notices that $\hat{O}_s^{\rm SC}$ is different from the superconducting order parameters proposed previously for the armchair CNTs [34]. This is because the band structure is different: the interband order parameter, that was previously prohibited due to the conservation of $k_\parallel$, now is allowed because in zigzag(like) tubes the chains of ladder are associated with valleys and Dirac cones are located at $K_\parallel = 0$. Moreover, if the circumferential momentum is conserved, then by requiring $\vec{k}_1 = -\vec{k}_2$ within the BCS pair, we find that indeed the interchain (intervalley) $O_s^{\rm SC}$ is favored (see Appendix for details). Moreover, from a basic symmetry argument, we know that the intervalley Andreev reflection is protected (versus for instance disorder) by time-reversal symmetry. On the other hand, the intravalley pairing would be protected by the so-called symplectic symmetry, but this one is already broken from the very beginning by introducing the $\Delta_{\rm SO}$.

So far, we have discussed the relation between $\hat{O}_{s,m}^{\rm SC}$ and and other uniform SC orders proposed before. A novel aspect of proximity effect, that is inevitably present in chiral tubes, is its nonuniformity. For a chiral tube that is rolled along the helical line one may consider the skew turn to be a built-in rotation angle versus substrate lattice. Since strength of bonding is related to interatomic distance, the de Moire pattern of the substrate-tube hybridization appears and the proximity effect is no longer uniform but instead it becomes periodic [35] (see Appendix for details). Such periodic proximity effect is favorable for more exotic SC orders proposed [36] for the two-leg ladder models and known as pair density waves. One defines a composite order parameter [36], that is a product of the $\hat{O}_{s,m}^{\rm SC}$ and some density wave. The density wave shall be defined in the intravalley channel to avoid a direct competition with superconductivity. One advantage is that one can construct an operator $O_{\rm PDW}^{\rm SC}$ which, albeit less relevant, depends only on $\phi_{\sigma+}$ in the spin sector. This allows to avoid a potential problem if a field $\phi_{\sigma-}$ is after all locked. The SC

order most likely retains a topologically trivial character, in the sense that standard procedure of Ref. [36] again favors $\hat{O}_s^{\rm SC}$. There are many other fascinating aspects of nonuniformity that should stimulate research in this direction. One is that the SC proximity effect shall be particularly strong for a chemical potential for which $k_{dM} = k_F$. This opens an exciting perspective of gate tuning of SC order in CNTs.

C. Other symmetry-breaking terms; valley mixing

For completeness, we comment on other backscattering operators, analogous to H_{di} and $H_{\rm SO}$, that can be introduced into the Hamiltonian of a CNT. One frequently proposed perturbation is an intervalley backscattering, the so-called $\Delta_{KK'}$. No matter what the content in the spin space we choose, this operator written in bosonic language contains $\theta_{\rho-}$ field, a field canonically conjugate to all cosine terms present in Eqs. (5)–(7). This means that $\Delta_{KK'}$ is quickly suppressed by all other terms as one is moving along the RG trajectory (towards $L \to \infty$ in quantum dot language). Moreover, even in the case when an extremely strong $\Delta_{KK'}$ is able to dominate the physics, since the pairing operators in Eqs. (23) and (24) contain $\cos\phi_{\rho-}$ then none of these (including the potentially topologically nontrivial, nonlocal $\hat{O}_m^{\rm SC}$) shall be favored. It seems that the $\Delta_{KK'}$ reduces the propensity of the system to any standard proximity effect.

One can also ask an opposite question: What symmetry-breaking term could potentially support the $\hat{O}_m$ order? A brief inspection of all order parameters reveals that this is a rather exotic spiral electric field acting opposite on two valleys (but valley diagonal), however, this would need to be taken together with attractive $V(q \approx 2|K|)$ interactions.

VI. CONCLUSIONS

We have shown that, for a chosen subset of CNTs, the presence of spin-orbit coupling $\Delta_{\rm SO}$ leads to a gap opening in the spectrum of two bosonic modes $\phi_{\rho-}$ and $\phi_{\sigma+}$. This drastically reduces the subset of proximity effects allowed at the lowest energies: we find that only a phase with a trivial topology is allowed. This statement is quite general as it should remain valid also upon increasing the interaction strength, doping, hybridization with the substrate, and upon adding another symmetry-breaking term $\Delta_{KK'}$. An extra motivation, and a broader perspective, for this work comes from the recently synthesized 2D analogs of graphene: silicene, germacene, and stanene. This gives a hope for a new class of nanotubes that shall be built out of atoms heavier than carbon. Since $\Delta_{\rm SO} \sim \lambda_{\rm SO}$ (where $\lambda_{\rm SO}$ is an atomic spin-orbit coupling constant [11]), then the fine effects predicted here can become orders of magnitude larger.

APPENDIX A: ESTIMATE FOR $\langle\cos\tilde{\phi}_{\rho+}\rangle|_{\omega=\Lambda'}$

The dynamics of the fast field $\phi_{\rho+}(x)$ for energies $\sim\Lambda'$ is rather complicated. Usually $\delta \sim 1$ implies that the g_d and $g_{\rm SO}$ terms rapidly drop out of the problem [and g_3 as well, but by writing Eq. (20) we had already neglected g_3]. However, already in the simplest single-mode sine-Gordon model, the issue of how precisely the expectation values disappear when δ becomes substantial has proven to be quite nontrivial and depends on how precisely RG procedure is set up [37]. Our model is much more complicated as the dynamic coupling with three other modes is present. For instance, in the argument of the cosine one can clearly see the competition between $\eta(x)$ and δx. Moreover, the amplitude of the cosine, that is $M[\phi_{i\neq\rho+}]$, shall have an extra increase when the two neutral fields order.

To tackle the problem, let us assume that, to begin with when $\eta(x) \approx 1$, $\eta(x)$ dominates. At Λ' energy scale the neutral fields still fluctuate, with a velocity that is irrational with the holon velocity, thus, $M[\phi_{i\neq\rho+}]$ and the $\eta(x)$ field can be considered as amplitude and phase of a complex random variable. Then, Eq. (20) can be interpreted as a model of a random backscattering in a TLL. The suppression of g_d is delayed by the fact that for the disorder problem, the scaling dimension is even larger $d_{\rm dis} = 3 - 2K_{\rho+}$. One can say that a strong enough disorder freezes the correlation function for $l \approx \Lambda'$. Such a phenomenon occurs also for incommensurate (not necessarily random) potentials when modes of different velocities couple. It is then known as Aubry-André transition [38]. The crossover is quite complex, but most likely as the energy scale l decreases during the RG, then $\eta \to 0$ (the fluctuations cease below the energy $\sim M_{\rho-}$), the randomness disappears and $g_{3,d,{\rm SO}}[l]$ resume their flow to zero, driven by a finite doping. However, for energies around Λ', the sine-Gordon model (20), with a finite, energy-independent amplitude of the cosine term, gives a correct description. Then, one can attempt to compute $\langle\cos\tilde{\phi}_{\rho+}\rangle|_{\omega=\Lambda'}$, in a limit when the shift goes to zero, by using results known from the Ising model in the renormalized classical regime. One may either use the zero-temperature result $\sim K_0(\tilde{g}_{1c}\tau')$, where K_0 is the modified Bessel function of the second kind and a characteristic time scale is set as $\tau' \sim 1/\Lambda'$, or a finite-temperature result [39] where $\langle\cos\phi_{\rho+}\rangle|_{\omega=\Lambda'}$ is proportional to $\mathrm{erfc}(\sqrt{\tilde{T}/2\tilde{g}_{1c}})$ with a characteristic temperature taken to be $k_B\tilde{T} = \Lambda'$ (and erfc is a complementary error function). In both estimates, we get $\langle\cos\phi_{\rho+}\rangle|_{\omega=\Lambda'} \sim 10^{-1}$. We consider it as an upper limit for $\langle\cos\tilde{\phi}_{\rho+}\rangle|_{\omega=\Lambda'}$ and in all further calculations we take a more conservative value $\langle\cos\tilde{\phi}_{\rho+}\rangle|_{\omega=\Lambda'} = 10^{-2}$.

APPENDIX B: DETAILS OF AN OVERLAP WITH A SUBSTRATE

In Ref. [40], it is shown that every site which is in touch with a superconductor, upon integrating out the BCS condensate, acquires an emergent pairing potential: $\int dx\,dy\,\Delta_{\rm SC}(x,y)[c^\dagger_\sigma(x,y)c^\dagger_{-\sigma}(x,y) + \text{H.c.}]$ where (x,y) are the site coordinates (interface has 2D character) and $\Delta_{\rm SC}(x,y) \sim t''(x,y)^2/V_F$ is a pairing strength, with $t''(x)$ a hybridization between CNT and a substrate. Let us consider a process of creation of a Cooper pair inside a CNT: $c^\dagger_{\vec{k}_1}c^\dagger_{\vec{k}_2}$. For a moment we need to take a 2D $\vec{k}_1$ because we keep interfaces' 2D character. When the pair is created in two different valleys (an intervalley term), it is compatible with the standard s-wave BCS pairs in the substrate where $k_1 = -k_2$. Contrarily, the intravalley term does not conserve momenta since then $k_{1\perp} = k_{2\perp} \pm 2K_\perp$. Thus, this second process will be suppressed when $k_{i\perp}$ is a conserved quantity during the tunneling process.

We can try to quantify the condition for conservation of the circumferential momenta. We take the hybridization $t''(x,y)$ to be a Gaussian with a width proportional to the nanotube radius: $\delta y = \alpha_b R$, where α_b is some proportionality constant and y is a direction along the tube's circumference. This relation simply encodes the fact that for broader tubes, there are more carbon atoms that can build a covalent bond with a substrate. Finite δy produces a momentum resolution $\delta k_{\text{perp}} \approx 1/\delta y$. The two valleys can be distinguished provided the real-space Gaussian is broad enough, that is, $\delta k_{\text{perp}} < |K| \Leftrightarrow R > a/|K|$. When this condition is fulfilled, one can consider valley index and thus $k_\perp$ to be a conserved quantity in a substrate-CNT tunneling process.

The microscopic model also allows us to take a closer look at the nonuniformity of the $t''(x)$. For a chiral tube, the hexagonal lattice makes consecutive skew turns around the central axis of the tube. Then, looking from the top it is very much like a sequence of tilted hexagons ($\delta y > \sqrt{3}a$, with a graphene lattice constant, is assumed). If one puts two hexagonal lattices one on top of another and rotate (or rescale) one of them, then one obtains the periodic de Moire pattern. Rescaling is necessary only when the substrate is a crystal different from graphene. We conclude that a chiral CNT placed on the top of a 2D surface gives an effective hybridization $t''(x) = \frac{1}{\delta y}\int dy\, t''(x,y)$ that is not constant along the tube but varies, and these variations are the strongest for smaller tubes where the effect is not averaged out by integration over large δy. For scaling factor between two lattices equal to one (e.g., both based on graphene), one finds [35] that the angle between the $\vec{k}_{dM}$ and the CNT basis is $\pi/2$ and indeed the hybridization $t''(x)$ along the 1D profile is periodic. The patterns' periodicity depends on the chiral angle, for small chiral angles very small $|\vec{k}_{dM}|$ can be reached.

[1] Liang Fu and C. L. Kane, Superconducting Proximity Effect and Majorana Fermions at the Surface of a Topological Insulator, Phys. Rev. Lett. **100**, 096407 (2008).

[2] Satoshi Fujimoto, Topological order and non-abelian statistics in noncentrosymmetric s-wave superconductors, Phys. Rev. B **77**, 220501 (2008).

[3] Frank Wilczek, Majorana returns, Nat. Phys. **5**, 614 (2009).

[4] Jason Alicea, Majorana fermions in a tunable semiconductor device, Phys. Rev. B **81**, 125318 (2010).

[5] V. Mourik, K. Zuo, S. M. Frolov, S. R. Plissard, E. P. A. M. Bakkers, and L. P. Kouwenhoven, Signatures of Majorana fermions in hybrid superconductor-semiconductor nanowire devices, Science **336**, 1003 (2012).

[6] Dmitry Bagrets and Alexander Altland, Class d Spectral Peak in Majorana Quantum Wires, Phys. Rev. Lett. **109**, 227005 (2012).

[7] Jie Liu, Andrew C. Potter, K. T. Law, and Patrick A. Lee, Zero-Bias Peaks in the Tunneling Conductance of Spin-Orbit-Coupled Superconducting Wires with and without Majorana End-States, Phys. Rev. Lett. **109**, 267002 (2012).

[8] Suhas Gangadharaiah, Bernd Braunecker, Pascal Simon, and Daniel Loss, Majorana Edge States in Interacting One-Dimensional Systems, Phys. Rev. Lett. **107**, 036801 (2011).

[9] C. L. Kane and E. J. Mele, Size, Shape, and Low Energy Electronic Structure of Carbon Nanotubes, Phys. Rev. Lett. **78**, 1932 (1997).

[10] T. Ando, Spin-orbit interaction in carbon nanotubes, J. Phys. Soc. Jpn **69**, 1757 (2000).

[11] Jae-Seung Jeong and Hyun-Woo Lee, Curvature-enhanced spin-orbit coupling in a carbon nanotube, Phys. Rev. B **80**, 075409 (2009).

[12] R. Egger and K. Flensberg, Emerging dirac and majorana fermions for carbon nanotubes with proximity-induced pairing and spiral magnetic field, Phys. Rev. B **85**, 235462 (2012).

[13] J. D. Sau and S. Tewari, Topological superconducting state and majorana fermions in carbon nanotubes, Phys. Rev. B **88**, 054503 (2013).

[14] Charles Kane, Leon Balents, and Matthew P. A. Fisher, Coulomb Interactions and Mesoscopic Effects in Carbon Nanotubes, Phys. Rev. Lett. **79**, 5086 (1997).

[15] R. Egger and A. O. Gogolin, Correlated transport and non-fermi-liquid behavior in single-wall carbon nanotubes, Eur. Phys. J. B **3**, 281 (1998).

[16] F. Kuemmeth, S. Ilani, D. C. Ralph, and P. L. McEuen, Coupling of spin and orbital motion of electrons in carbon nanotubes, Nature (London) **452**, 448 (2008).

[17] T. S. Jespersen, K. Grove-Rasmussen, K. Flensberg, J. Paaske, K. Muraki, T. Fujisawa, and J. Nygård, Gate-Dependent Orbital Magnetic Moments in Carbon Nanotubes, Phys. Rev. Lett. **107**, 186802 (2011).

[18] Vikram V. Deshpande, Marc Bockrath, Leonid I. Glazman, and Amir Yacoby, Electron liquids and solids in one dimension, Nature (London) **464**, 209 (2010).

[19] Andreas Schulz, Alessandro De Martino, and Reinhold Egger, Spin-orbit coupling and spectral function of interacting electrons in carbon nanotubes, Phys. Rev. B **82**, 033407 (2010).

[20] Sam T. Carr, Alexander O. Gogolin, and Alexander A. Nersesyan, Interaction induced dimerization in zigzag single wall carbon nanotubes, Phys. Rev. B **76**, 245121 (2007).

[21] Alex Kleiner and Sebastian Eggert, Band gaps of primary metallic carbon nanotubes, Phys. Rev. B **63**, 073408 (2001).

[22] Magdalena Marganska, Piotr Chudzinski, and Milena Grifoni, The two classes of low-energy spectra in finite carbon nanotubes, Phys. Rev. B **92**, 075433 (2015).

[23] M. Tsuchiizu, P. Donohue, Y. Suzumura, and T. Giamarchi, Commensurate-incommensurate transition in two-coupled chains of nearly half-filled electrons, Eur. Phys. J. B **19**, 185 (2001).

[24] P. Chudzinski, M. Gabay, and T. Giamarchi, Orbital current patterns in doped two-leg Cu-O hubbard ladders, Phys. Rev. B **78**, 075124(2008).

[25] A. A. Nersesyan and A. M. Tsvelik, Coulomb blockade regime of a single-wall carbon nanotube, Phys. Rev. B **68**, 235419 (2003).

[26] L. S. Levitov and A. M. Tsvelik, Narrow-Gap Luttinger Liquid in Carbon Nanotubes, Phys. Rev. Lett. **90**, 016401 (2003).

[27] E. D. Minot, Y. Yaish, V. Sazonova, and P. McEuen, Determination of electron orbital magnetic moments in carbon nanotubes, Nature (London) **428**, 536 (2004).

[28] A. O. Gogolin, A. A. Nersesyan, and A. M. Tsvelik, *Bosonization and Strongly Correlated Systems*, 1st ed. (Cambridge University Press, Cambridge, UK, 1998).

[29] Michele Fabrizio, Alexander O. Gogolin, and Alexander A. Nersesyan, From Band Insulator to Mott Insulator in One Dimension, Phys. Rev. Lett. **83**, 2014 (1999).

[30] P. M. Singer, P. Wzietek, H. Alloul, F. Simon, and H. Kuzmany, NMR Evidence for Gapped Spin Excitations in Metallic Carbon Nanotubes, Phys. Rev. Lett. **95**, 236403 (2005).

[31] Balázs Dóra, Miklós Gulácsi, Ferenc Simon, and Hans Kuzmany, Spin Gap and Luttinger Liquid Description of the NMR Relaxation in Carbon Nanotubes, Phys. Rev. Lett. **99**, 166402 (2007).

[32] D. V. Khveshchenko and T. M. Rice, Spin-gap fixed points in the double-chain problem, Phys. Rev. B **50**, 252 (1994).

[33] Annica M. Black-Schaffer and Sebastian Doniach, Resonating valence bonds and mean-field d-wave superconductivity in graphite, Phys. Rev. B **75**, 134512 (2007).

[34] Karyn Le Hur, Smitha Vishveshwara, and Cristina Bena, Double-gap superconducting proximity effect in armchair carbon nanotubes, Phys. Rev. B **77**, 041406 (2008).

[35] Klaus Hermann, Periodic overlayers and Moire patterns: Theoretical studies of geometric properties, J. Phys.: Condens. Matter **24**, 314210 (2012).

[36] Akbar Jaefari and Eduardo Fradkin, Pair-density-wave superconducting order in two-leg ladders, Phys. Rev. B **85**, 035104 (2012).

[37] B. Horovitz, T. Bohr, J. M. Kosterlitz, and H. J. Schulz, Commensurate-incommensurate transitions and a floating devil's staircase, Phys. Rev. B **28**, 6596 (1983).

[38] Serge Aubry and Gilles André, Analyticity breaking and Anderson localization in incommensurate lattices, Ann. Israel Phys. Soc. **3**, 18(1980).

[39] Subir Sachdev, Universal, finite-temperature, crossover functions of the quantum transition in the Ising chain in a transverse field, Nucl. Phys. B **464**, 576 (1996).

[40] Ian Affleck, Jean-Sébastien Caux, and Alexandre M. Zagoskin, Andreev scattering and Josephson current in a one-dimensional electron liquid, Phys. Rev. B **62**, 1433 (2000).